Microwave Holography: Applications and Techniques

G. TRICOLES, MEMBER, IEEE, AND NABIL H. FARHAT, SENIOR MEMBER, IEEE

Abstract—**The techniques and applications of microwave holography are described. The connections with related fields, acoustical holography, and quasi-holography are summarized.**

I. Introduction

HOLOGRAPHY first gained the attention of scientists when it was demonstrated as a two-step imaging process. It later gained widespread attention because it produced remarkably lifelike three-dimensional images. Subsequent research and development led to the application of holographic techniques for data processing and nondestructive testing. Recent work, combining holographic methods with acoustic waves and microwaves, has given new insights into wave phenomena with significant potential for instrumentation and measurement, information collection, wave propagation, and object identification. This paper surveys microwave holography, its techniques, and its applications.

In the first of the two steps basic to holography, a coherent wave illuminates an object and scatters a field onto a detector (such as photographic film for light waves). A portion of the illuminating wave that bypasses the object also illuminates the film to produce an interference pattern, which the film records. Images are then formed in the second step when the developed film transparency, a hologram, is illuminated with coherent light. The hologram diffracts two waves, one proportional to the object-scattered field and another proportional to its complex conjugate. Both waves form images, but they can overlap and obscure each other. This overlap was a disadvantage to holography for several years until Leith and Upatneiks introduced a new experimental technique; since then, holography has grown rapidly.

Gabor originated holography when he proposed the method to increase the resolution of electron microscopes [1]. Although Gabor demonstrated the feasibility of holography with light, it has not yet improved electron microscopes. However, the two-step method has significantly influenced optics. The method provides an indirect means of recording the phase of optical wavefronts, since photographic film responds to intensity but not to complex amplitude. Holography is remarkable because it provides an interval between the two steps. The interval is useful for processing and analyzing the data stored in the hologram. Some terminology is now common. The wave that bypasses the object is the reference wave; it is coherent with the wave that illuminates the object. The first of the two steps is the hologram formation step; the second, the wavefront reconstruction step.

Holograms and wavefront reconstruction have become significant for optics since Leith and Upatnieks introduced their experimental technique in which the reference wave is a distinct beam, produced by a beam splitter and inclined to the beam from the object [2]. The technique separates the overlapping images produced in Gabor's original arrangement, in which the reference and object waves are nearly parallel. Aside from imaging, optical holography has many applications and the field is well documented [3]–[8].

Acoustical holography is an active field [9]–[15] with many similarities to microwave holography because the wavelengths employed in the two fields differ by about one order of magnitude. An analysis of scanning techniques for acoustical holography has provided data useful for microwave holography [16].

In this paper we describe what Leith terms true microwave holography rather than quasi-microwave holography [17]. The latter utilizes pulsed radiation to measure range and doppler records to measure azimuth, but true holography utilizes measurements over a two-dimensional area. In true holography, image coordinates are two orthogonal distances, both orthogonal to radial distance; in quasi-holography, one of the coordinates is range. Because we omit quasi-holography, we omit synthetic aperture radar (SAR), which forms one-dimensional holograms. Those interested in SAR can consult extensive available literature [18]–[20].

The second section of this paper describes the formation of microwave holograms. The measured quantities, data collection techniques, and data storage are described.

The third section describes experimental reconstruction methods, with light and microwaves, along with computed reconstructions. The final section describes applications.

The ability of microwaves to propagate through optically opaque dielectrics makes microwave holography useful for testing dielectric structures for anomalies. Examples include the inspection of laminated plastic parts, such as radomes, and archeological exploration. Furthermore, it is useful in diagnostic work on antennas and radomes, and for studying the propagation of radio waves through the atmosphere. It may become useful also for plasma diagnostics.

II. Hologram Formation

A. Measurement

Hologram formation means detecting the phase and amplitude of the field scattered by the object and storing the data. The measured quantity can be intensity, but at microwave frequencies both phase and amplitude (square root of intensity) can be measured. Intensity alone is often also observed because the apparatus is simpler than that required to measure both phase and amplitude.

Hologram measurements require a reference field coherent with the wave that the object scatters. The coherent reference is required to obtain the object wave's phase, which is necessary for reconstructing the object wave and forming images. To describe the measurements we utilize scalar notation be-

Manuscript received February 20, 1976; revised July 22, 1976.

G. Tricoles is with the General Dynamics Electronics Division, P.O. Box 81127, San Diego, CA 92138.

N. H. Farhat is with the Moore School of Electrical Engineering, University of Pennsylvania, Philadelphia, PA 19174.

cause in many cases the field is linearly polarized, and holograms are usually flat. Let a complex-valued field component from the object be u_o; let u_r be the component from the reference wave source. Then the complex-valued field on the measurement surface (the hologram recording plane) is

$$u_h = u_o + u_r. \tag{1}$$

The intensity is

$$|u_h|^2 = u_h u_h^* \tag{2}$$

where * denotes complex conjugation. To make phases explicit let u_o be $a_o \exp i\phi_o$ and u_r be $a_r \exp i\phi_r$. From (2) we see that

$$|u_h|^2 = a_o^2 + a_r^2 + a_o a_r \exp [i(\phi_o - \phi_r)] + a_o a_r \exp [-i(\phi_o - \phi_r)]. \tag{3}$$

Equation (3) shows that ϕ_o, the phase of the object wave, is implicit in the observable values of $|u_h|^2$, which represents a pattern of intensity fringes. The effect of phase variations is to modulate fringe positions. These relationships were first suggested by D. Gabor.

Detectors for intensity measurements are categorized in two classes; one includes discrete antennas and receivers, the other includes continuous materials that change under microwave illumination.

Liquid crystal films and Polaroid film are examples of continuous detectors. Liquid crystals can be utilized because they change color with temperature. The liquid crystal is applied to a layer that absorbs incident microwave energy, which heats the crystal, changing its color. Subsequent photographic reduction of the displayed color patterns through colored filters produces black and white holograms suitable for reconstruction with laser light. Liquid crystals have been utilized by Augustine *et al* [21], [22], Stockman and Zarwyn [23], and Iizuka and Gregoris [24]. Kock suggested real-time imaging of concealed objects without reconstruction; a liquid crystal film would record the scattered field near an object to obtain its geometric projection [25]. Although liquid-crystal detectors are feasible, their sensitivity is low. Intensity levels must be about 10 mW/cm^2, orders of magnitude higher than crystal diodes require. Iizuka has utilized Polaroid film [26] by illuminating the film with microwaves after exposing it to white light to start the development process. The microwaves heated the film and changed the development rate so that variations in microwave intensity produced distinct colors. Here again sensitivity is low, of the order of ten milliwatts per square centimeters.

The intensity scattered by an object can be measured by an array of antennas with crystal diode detectors; however, an array is expensive, so data often are measured by mechanically scanning an area with one antenna. Of course, scanning causes delays. Delays are undesirable because instrument or source instabilities cause errors. Delays are unacceptable for recording transient events. Nevertheless, scanning is adequate for laboratory measurements utilized in nondestructive testing and similar situations where the wavefronts being recorded do not change in time.

Single antennas have been scanned in several ways. Linear motion on a series of parallel lines is common [27]–[31]; see Fig. 1 for example. Parallel arcs have been used by placing the antenna on an arm with fixed radius from a center that is laterally displaced [32]–[34]. Farhat and Guard utilized a spiral path, by rotating an arm about a fixed center and decreasing the radius during the rotation [35]; see Fig. 2. Double circular scans have also been considered [36] to accelerate mapping of microwave fields over an aperture of 1 m diameter.

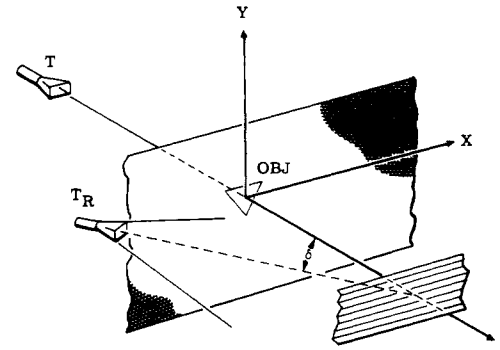

Fig. 1. Experimental arrangement with coplanar object and reference source. The object (OBJ) was a triangular aperture in an absorbing screen, at the plane $Z = 0$. An antenna T radiates a beam to illuminate the object, and another reference antenna readiates a reference beam coherent with the illuminating beam. Both radiated beams were produced by the same Klystron source, which was connected to a directional coupler, a form of beamsplitter. A small receiving antenna was moved with the center of its operation on each of the horizontal lines that lie in a plane parallel to the object. This scanning plane is the hologram plane.

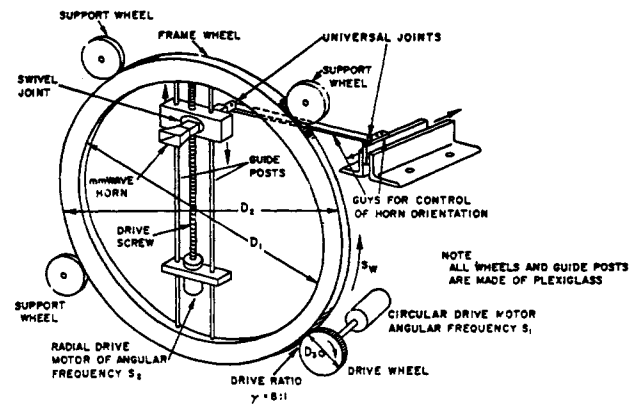

Fig. 2. Spiral scanner.

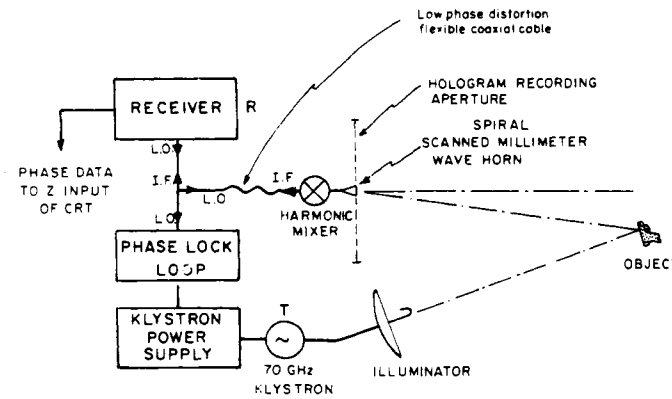

Fig. 3. Superheterodyne receiver arrangement utilizing local oscillator as reference source.

Measurements of both phase and amplitude require a receiver that is more complex than an intensity detector; see Fig. 3. However, when only intensity is measured, sampling theory shows that the distance between adjacent samples must

be half that for phase and intensity measurements. The intuitive reason is that a measurement of phase and intensity gives two real numbers; intensity measurement gives one. Criteria for sampling have been discussed by Lohmann [37].

The simplest experimental arrangement is that shown in Fig. 1. A receiving antenna scans while the transmitting antenna, the reference antenna, and the object remain stationary. A diode detector or receiver measures the intensity distribution formed by interfering object and reference beams. Although economical, a radiated reference beam has the disadvantage that it can be scattered by the surroundings or the probe support leading to distortions in the reference field. To avoid this problem the reference wave can be directed to the detector through waveguide. This choice usually requires additional equipment, rotating joints, or flexible cables to convey the reference signal to the detector or mixer. It also requires a phase shifter to change phase linearly with probe motion to simulate an inclined reference beam. Orme and Anderson shifted the phase of the reference wave by radiating it from an antenna toward a reflecting plane and receiving the reflected wave with an antenna that moved with the scanning probe [38]. Fig. 3 shows an arrangement that uses a flexible cable for conveyance of the reference wave.

Measurements can be accelerated by scanning a linear array of antennas and crystal detectors over the recording aperture. Fig. 4 shows an array that has 16 antennas and crystal detectors. The array is translated in the direction perpendicular to its length to map the hologram data in a rectangular aperture.

An approach that compromises between cost and speed utilizes two crossed linear arrays. This approach was suggested by Wells for acoustical holography [39]. Fig. 5 shows a microwave array that samples the wavefront and, in contrast to a phased array, does not form a narrow beam [40]. It has a vertical array of 16 transmitting antennas and a horizontal array of 16 receiving antennas. Each transmitting antenna is connected to a continuous wave source through a set of mechanical waveguide switches. Only one antenna radiates at any instant. The receiving antennas are connected sequentially to a phase and intensity receiver through mechanical waveguide switches while one antenna of the transmitting array radiates. The sequence is repeated for each transmitting antenna to generate 256 complex-valued samples in 30 s. The frame time is limited by the data logger and the mechanical switches, but it can be reduced by using a receiver at each antenna of the receiving array and with electronic rather than mechanical waveguide switches.

There are advantages to simultaneously scanning the transmitting and receiving antennas as a unit. The apparatus is simplified because no flexible connection is required for the reference field. Furthermore, the object is illuminated from diverse directions so the image is less specular. The resolution is improved by a factor of two because the phase of the object wave changes at twice the rate obtained when one antenna scans. This increased phase rate and improved resolution are well known in the SAR field. Simultaneous scanning has been demonstrated in acoustical holography by Hildebrand and Haines [16]. It has also been utilized in microwave holography [38], [41], [42]. An example is given in Section III-C.

B. Encoding

Consider a single scanning antenna. If intensity is measured, the fringe pattern can be displayed conveniently and inex-

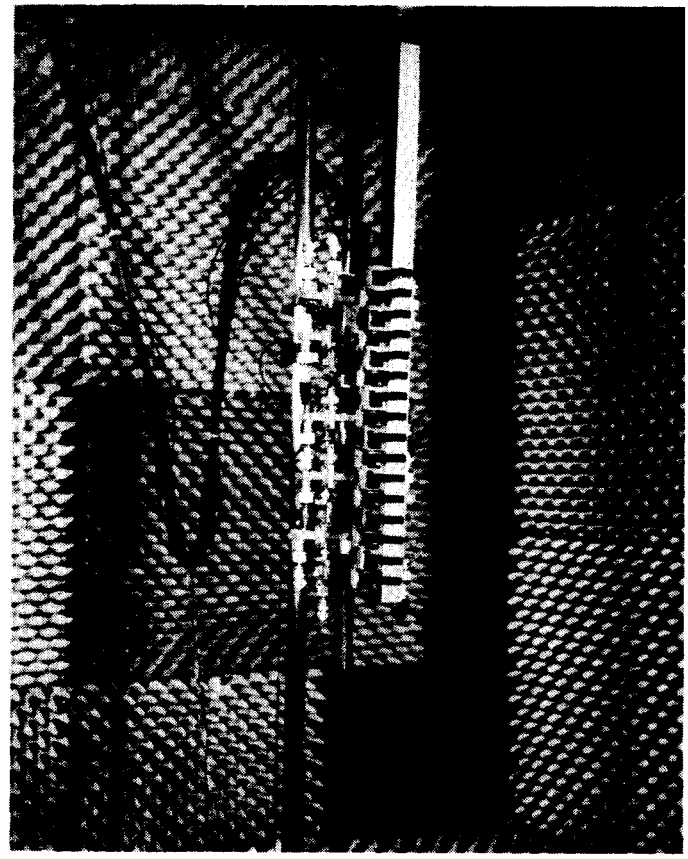

Fig. 4. Linear array for intensity measurements. The array is translated horizontally to scan an area.

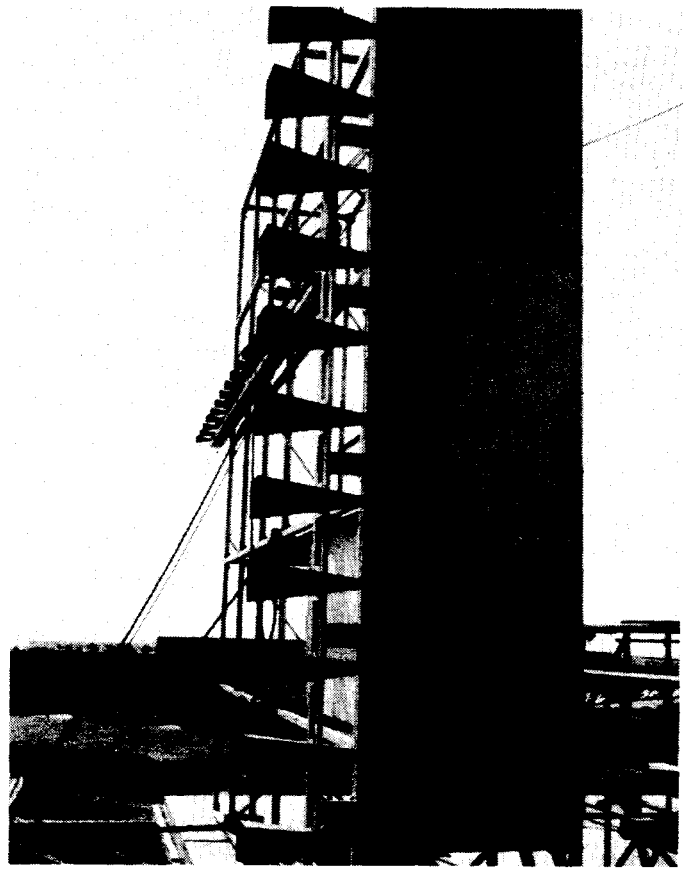

Fig. 5. Crossed linear arrays.

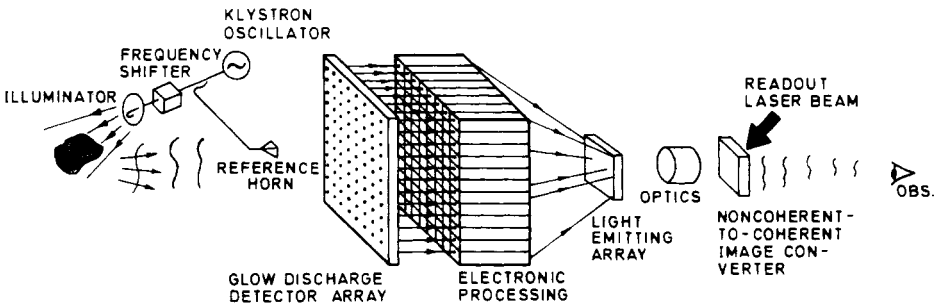

Fig. 6. Concept of real-time microwave holographic camera employing complete parallel processing.

pensively by an oscilloscope [27], [33]. The detected voltage, proportional to microwave intensity, modulates the electron beam and the spot brightness. The beam is moved synchronously with the probe by a servomechanism. If phase is measured, fringes can be formed by modulating the brightness with a voltage proportional to phase [35]. If phase and amplitude are measured, both quantities can be displayed by forming detour phase holograms with an oscilloscope [43]. In all these cases, the oscilloscope displays are photographed and size reduced to form transparencies that are holograms. Images are produced by illuminating the holograms with laser light. In some early work, Kock displayed fringes with a lightbulb and photographed the bulb as it scanned the field [44].

Although an oscilloscope display is convenient for a single probe, it is not suitable for use with linear array of receiving antennas since an array would require a multiple beam oscilloscope or multiplexing the array output and displacing the oscilloscope beam. It is simpler to utilize a linear array of light sources, using a source for each antenna and detector. The voltages from the detector are amplified to control the brightness of the source. A time exposure photograph of the array of light sources is made while a linear array is scanned in the direction perpendicular to its length. Dynamic range is limited. In our work we were able to produce reasonable images from holograms with only 6-dB variations in intensity of microwave fringes.

Microwave holograms can be formed by measuring fringe patterns and using them as guides for fabricating holograms consisting of metallic scatterers or absorbing material. The next section shows an example and cites others. Phase data can also be utilized to form phase holograms by contouring dielectrics. Microwave hologram data also can be digitized for computer processing. For the lower microwave frequencies, digital processing is superior to experimental reconstruction with light because it eliminates the scaling problem. For shorter millimeter waves the production of an optical hologram requires less scaling; however, the original fringes can be more closely spaced than they are for centimeter waves in some experiments.

A new concept for a real-time holographic camera is shown in Fig. 6. The camera combines a two dimensional hologram recording array of sensors with real-time optical reconstruction scheme that will be discussed in more detail in Section III. The sensor array converts the intensity distribution in the hologram fringe pattern into electronic, intermediate frequency signals that are amplified and processed in parallel, and used to activate an array of light emitting diodes. In this fashion instantaneous visualization of the microwave hologram fringe pattern can be accomplished. Glow discharge detectors [45] are particularly suited for experimental hologram recording arrays because of their extremely low cost, their wide spectral response (covering the microwave and millimeter wave range), and because they function as an antenna and transducer simultaneously.

III. Wavefront Reconstruction

Because a hologram contains information derived from the Fraunhofer or Fresnel wavefields diffracted by the object, wavefront reconstruction and image retrieval can be described by Fourier transform operations. These operations can be performed either experimentally, say with an analog optical computer that may utilize the Fourier transform property of a convergent lens, or digitally by a computer, usually employing fast Fourier transform (FFT) algorithms. Both methods have advantages and disadvantages that make one better suited than the other, depending on the application. The advantages of optical computing include relative simplicity and instantaneous parallel processing of two-dimensional input data at the speed of light. The limitations of optical computing, on the other hand, stem from the slow rates at which data can be put into the computer, usually by means of photographic film. However, the development of recyclable light valves that can perform the function of the photographic film may remove this limitation [46]. Digital computing has the advantage of flexible processing, but it can only handle the data serially. Although the cost of nearly real-time digital computation of hologram data may be high, the availability of dedicated minicomputers and microprocessors is cutting such costs rapidly. In this section, both methods of wavefront reconstruction are discussed and examples of both types presented.

A. Experimental Reconstruction

The most common optical procedure utilizes a laser beam to illuminate an optical replica of the microwave hologram data [27]–[35]. This procedure has the advantage of giving visible images, which can be viewed and photographed. However, unless special optical arrangements are employed, the images are small and longitudinally distorted. The size and distortion problems arise because the microwave hologram cannot be adequately demagnified. The scale reduction should be in the ratio of the microwave and optical wavelengths, which is 3×10^4 for 1.8-cm waves and 6328-Å laser light [47], [48].

Such reduction factors mean that the hologram fringe pattern collected over a recording aperture one meter in diameter must be stored on a photographic film area less than one millimeter in diameter. The fringe density in such an optical halogram replica would necessitate the use of high resolution film in conjunction with complex optical reduction proce-

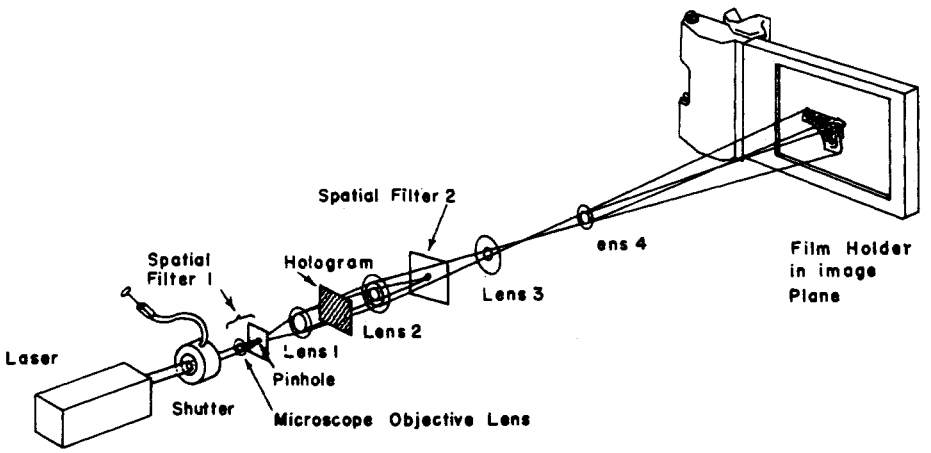

Fig. 7. Optical wavefront reconstruction.

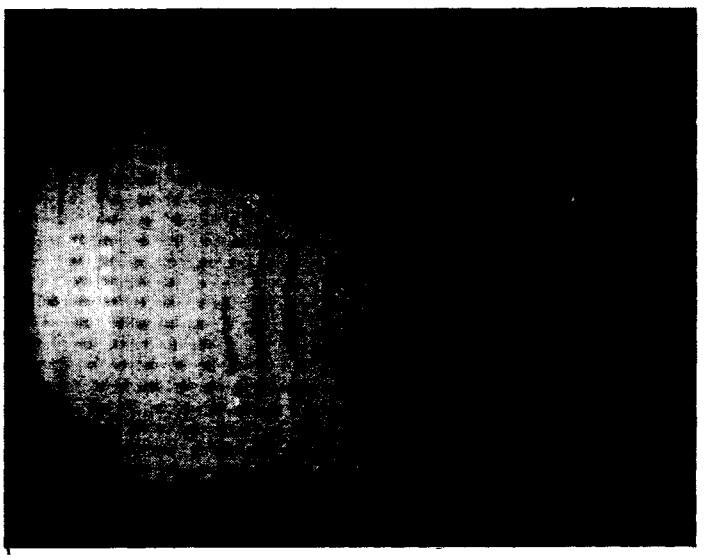

Fig. 8. Microwave hologram formed for object in Fig. 1.

dures. Fig. 7 shows an optical reconstruction arrangement designed to alleviate the scaling problem and the need for high resolution film [42]. The scheme involves optical reduction of the hologram transparency during reconstruction by means of lenses L_2 and L_3. Thus the size of the hologram transparency used need not be fractions of a millimeter, but can be relaxed to a few millimeters. This permits the use of lower resolution film or light valves for hologram data storage. The arrangement shown also permits the removal of background light in the image plane by insertion of a zeroth-order stop in the back-focal-plane, the Fourier transform plane, of lens L_2.

The problems caused by partial scaling suggested reconstruction with microwaves from full size holograms. Fig. 8 shows a microwave hologram formed with 1.87-cm microwaves in the arrangement of Fig. 1. The object was the triangular aperture in the plane screen that also contained the source of the reference beam. The hologram contains rectangular pieces of absorbing material with heights determined by the microwave intensity at interference minima.

Real-time optical reconstruction from previously formed microwave holograms employing a reusable liquid crystal-photoconductor (LC-PC) light valve is described by Wu and Farhat [49]. In their arrangement, shown in Fig. 9, the LC-PC light valve can be simultaneously optically addressed with non-

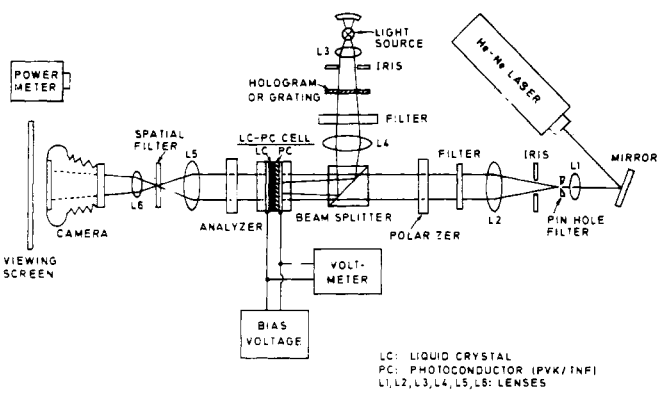

Fig. 9. Arrangement for rapid optical reconstruction with microwave holograms via a recyclable liquid crystal-photoconductor light valve.

coherent while light and readout with coherent He–Ne laser light for direct noncoherent-to-coherent image conversions.

Another approach to real-time reconstruction is based on spatially noncoherent optics. The method would include an areal antenna array to collect data for a Fourier transform hologram and an array of monochromatic light sources to display the received microwave intensity fringes. The light

sources are each coherent but not mutually coherent. The optical display is doubled by an interferometer, and the doubled pattern is optically Fourier transformed to form images. Although the spatially noncoherent reconstruction has been demonstrated feasible in laboratory experiments, a complete system has not yet been fabricated. This method requires no light valve.

B. Digital Computer Reconstruction

The characteristics of computer reconstructions are described in [50] and [51]. Computations eliminate the need for scaling. Computer reconstructions are potentially faster and more flexible than experimental reconstruction that utilizes tangible holograms because they eliminate the delay in making the hologram. Of course, light valves or spatially non-coherent reconstruction would operate in real time. Although high speed computation requires rather expensive apparatus, the development of minicomputers and FFT algorithms has simplified computational reconstruction. Examples are given in Subsection III-C.

C. Theory and Examples

This subsection gives theoretical descriptions of wavefront reconstruction and some examples. The theory helps to plan experiments and to interpret results; it also is the basis for computational reconstruction. The theory is approximate. Scalar diffraction theory is invoked since it is found adequate for many cases, and it is simpler than vector theory [31].

The arrangement in Fig. 1 is convenient. The formation step is simple, and reconstructions require simple diffraction, without lenses. Fig. 10 shows the essentials; the main feature is that the object and reference sources are equidistant from the hologram plane. Consequently the hologram fringes formed are uniformly spaced. The uniform spacing has led to the name lenseless Fourier transform holograms. Sometimes the arrangement is called the point reference method. It was utilized for optics first by Stroke. [4].

To analyze the hologram, suppose the object and reference waves are spherical and consider only the plane in Fig. 10. Let the field amplitude produced by the object wave in the hologram plane $x = x_h$ be $u_o = a_o \exp ikr_o$ and let the reference wave amplitude be $u_r = a_r \exp ikr_r$. The object has rectangular coordinates (x_o, y_o); the reference source is at (x_o, y_r). Therefore, under Fresnal conditions,

$$r_o = u + (y_h - y_o)^2 \, (2u)^{-1} \tag{4}$$

and

$$r_r = u + (y_h - y_r)^2 \, (2u)^{-1} \tag{5}$$

where u is $x_h - x_o$. Suppose intensity is recorded, and that an optical hologram is formed with transmittance proportional to intensity. The transmittance is

$$t = |u_o + u_r|^2 = a_o^2 + a_r^2 + a_o a_r \exp\,[ik(r_o - r_r)] + a_o a_r \exp\,[-ik(r_o - r_r)]. \tag{6}$$

Images are formed by illuminating the scale reduced hologram replica $t(m\, y_h)$ of equation (6) with the reconstructing wave u_c. Here m designates the scale reduction factor. From scalar diffraction theory the image amplitude is

$$u_i(x_i, y_i) = E \int t u_c \exp\,(ikr_i)\, dy_h \tag{7}$$

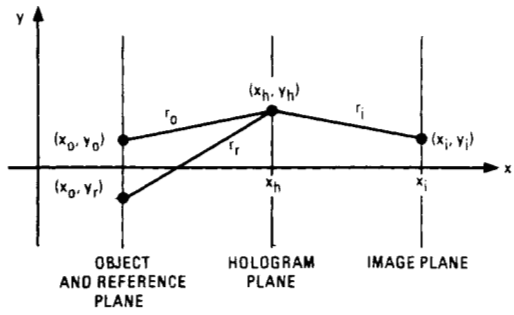

Fig. 10. Coordinates for point reference fourier transform hologram.

Fig. 11. Image of the object in Fig. 1 produced by illuminating the hologram in Fig. 8 with microwaves.

where E contains some phase factors and inverse distance factors. In the Fresnal approximation r_i is $v + (y_i - y_h)^2 \, (2v)^{-1}$, where $x = x_i$ is the position of the image plane and v is $x_i - x_h$. When equation (7) is evaluated, with t from (6), four terms arise. The first two come from the terms a_o^2 and a_r^2 in (6). They represent light that continues in the direction of the reconstructing beam; they do not produce an image because the phase data are absent from them. Images come from the third and fourth terms. In the third term, we see from (4) and (5) that:

$$r_o - r_r = (y_r - y_o)\, m y_h u^{-1} + y_o^2 - y_r^2 \, (2u)^{-1}. \tag{8}$$

Notice the quadratic terms in y_h are absent because the object and reference sources are coplanar. Let the reconstructing wave be a plane wave incident normal to the hologram; that is, $u_c = \exp ik' x_h$, where k' is $2\pi/\lambda'$ and λ' is the reconstruction wavelength. If the reconstruction is observed in the farfield, where $k' y_h^2 \ll 1$, then the quadratic term in y_h can be dropped from r_i, and the integration of (7) gives

$$u_i = H \operatorname{sinc} \{\pi H[(y_r - y_o)\, m\, (u\lambda)^{-1} - y_i (v\lambda')^{-1}]\} \tag{9}$$

where H is the height of the hologram.

The image is at $\hat{y}_i = (y_r - y_o)\, m(\lambda'/\lambda)\, (u/v)$. The symbol above y_i denotes the value determined by specific experimental conditions. The fourth term gives an image at $-\hat{y}_i$. Thus in optical reconstructions the hologram produces images in symmetric pairs about the undiffracted beam that is parallel to the illuminating beam. The images do not overlap. Although the preceding theory assumed spherical waves from point sources, the formulas for image locations describe holographic reconstruction of points of extended objects.

True microwave holography can be done with relatively simple equipment. The arrangement of Fig. 1 is an example. Fringes were measured and encoded into the hologram of Fig. 8, where the small rectangles are absorbing material. The local transmittance of each rectangle is proportional to the levels of microwave fringe intensity minima. Fig. 11 shows an image of

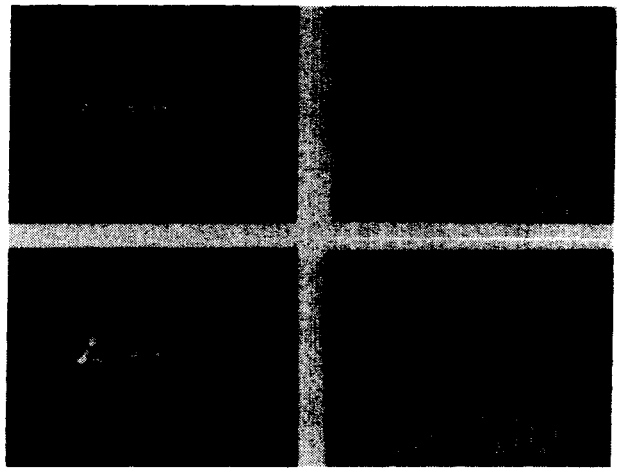

Fig. 12. Visible reconstructions of the triangular aperture in Fig. 1 and microscope photographs of holograms. The holograms differ in the exposures utilized in the photographic scale reduction. The upper hologram was exposed less than the lower. The correspondence between holograms and reconstructions is horizontal.

the triangular aperture. This image was formed by illuminating the hologram of Fig. 8 with spherical waves, wavelength 1.87 cm, and measuring the diffracted wave with a linear array of eight detectors. The detected intensity was displayed by an oscilloscope connected to the detectors through a sampling network. No lens was utilized for this microwave reconstruction.

Images of the triangular aperture were also formed with laser light. An optical hologram was produced from the microwave hologram, Fig. 8, by representing the absorbing regions with black regions on a white background and photographically reducing the binary representation. Fig. 12 shows the optical holograms and images produced by reconstruction with 6328-Å laser light. Image quality depends on the local transmittance of the hologram; exposure during the photographic reduction is a factor.

The images in Fig. 12 are described by (7), but two modifications are necessary. First, the integral is computed as a discrete sum because the data are sampled. The sampling produces higher order images. Although higher order images were not recorded by the photographs in Fig. 12, they were quite visible in the laboratory. The second modification results because the optical transmittance of the holograms is binary. For digital computations, the size of the small dots must be included in the integration. Fig. 13 shows examples of image intensity computed in the x-z plane of Fig. 1. The calculations were done first for all areas of the hologram and repeated with only 88 of the dots present. A series of such calculations was made to generate a two-dimensional image, which is shown in Fig. 14 for a threshold 23 dB below the on-axis intensity. The rapid intensity variations correspond to the speckle in Fig. 12.

The configuration utilized to produce the image in Fig. 11 from the microwave hologram in Fig. 8 differs from that for reconstruction with laser light. Scale reduction was unnecessary; moreover, the microwave reconstruction was done with spherical waves rather than a plane laser beam. The spherical wave is more convenient than a plane wave, for a small antenna can be utilized near the hologram to produce the reconstruction wave. For analysis the reconstruction spherical wave is written as $u_c = a_c \exp ikr_c$ in equation (7), where r_c is $w + (y_h - y_c)^2\ (2w)^{-1}$, with w being the distance of the reconstructing source from the hologram. From (7) with the focusing condition $v = -u$, the third term in (6) generates the image:

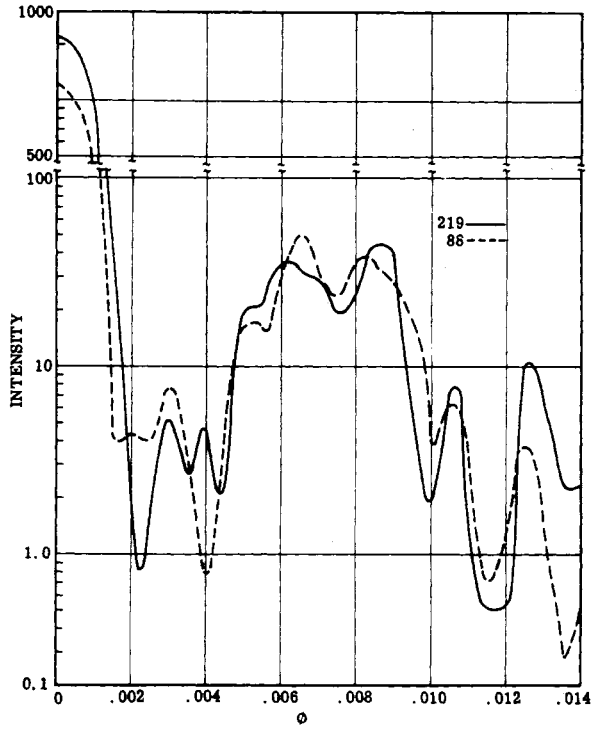

Fig. 13. Computed reconstruction for microwave data. The calculation was for the plane perpendicular to the hologram plane. The solid curve used data corresponding to all 219 rectangles in the hologram of Fig. 8, and the broken curve utilized data for the largest 88 rectangles.

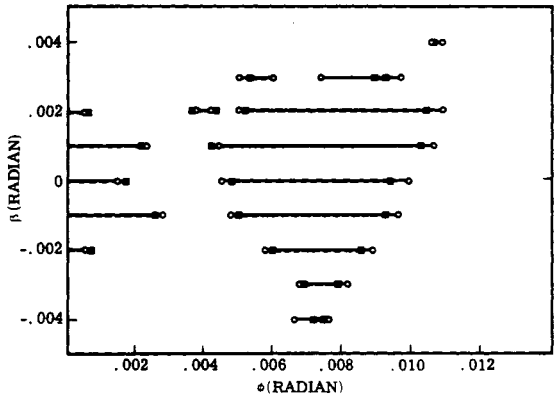

Fig. 14. Regions in which computed intensity exceeded the level 23 dB below on-axis maximum. The angle ϕ lies in the X-Z plane of Fig. 1; β is the polar angle from the Z-axis. Computations with 88 terms (0); with 219 (■).

$$u_i = E \int \exp\{ik[(y_h - y_c)u^{-1} - y_c w^{-1} - y_i v^{-1}]y_h\}\, dy_h$$
$$= \text{sinc}\{\pi H[(y_h - y_o)u^{-1} - y_c w^{-1} - y_i v^{-1}]\} \qquad (10)$$

The fourth term gives the same result except that the negative signs of the coordinates in the argument of the sinc function are positive. We see that a pair of images is formed. Since v is negative, the images are virtual (or true). The image shown in Fig. 11 is a second-order image at twice the off-axis angle of the first order; the first-order image was obscured by the diverging reconstruction wave.

For measurements of phase and amplitude, the field amplitude $u_o(x_h, y_h)$ produced by the object scattered wavefield

(a)

(b)

(c)

Fig. 15. Conventional scanned receiver holography. (a) Test object, (b) hologram, and (c) image.

represents the measured hologram data. In practice this data is available in sampled form. To simplify the following analysis we assume the data as continuous. Denote the object amplitude as $u_o(x_o, y_o)$. Application of scalar diffraction theory leads to the image amplitude:

$$u_i = E_p \int u_o(y_h) \exp\left[-i(\pi y_h^2/\lambda f) \exp\left\{ik[(y_i - y_h)^2/2v]\right.\right. dy_h\Big\} \tag{11}$$

where f is the focal length of a lens. If $u_o(y_h)$ is expressed as a diffraction integral over the object, we obtain

$$u_i = E_p' \iint u_o(y_o) \exp\left\{i[\pi\lambda^{-1} F y_h^2 - k(y_o u^{-1} + y_i v^{-1}) y_h]\right\} dy_o dy_h$$

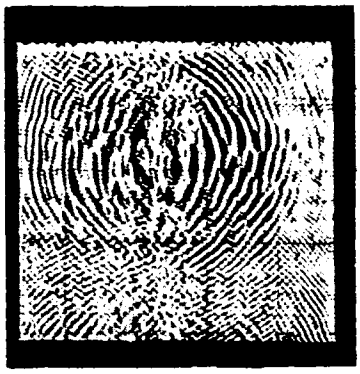

(a)

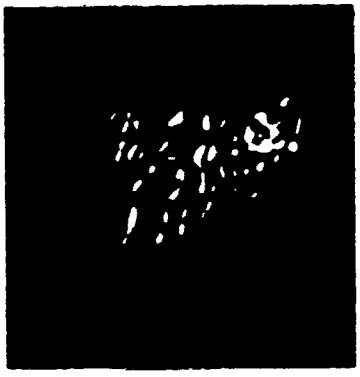

(b)

Fig. 16. Holography for simultaneously scanned receiver-Transmitter. The object is in Fig. 15, a) is the hologram, and b) is the image.

where F is $u^{-1} + v^{-1} + f^{-1}$, and E_p' has some phase factors and inverse distance factors. If we use the focusing condition $F = 0$, the simplified integral yields the image amplitude:

$$u_i = u_o(-uv^{-1} y_i). \tag{12}$$

From equation (12), the image is an inverted and scaled (demagnified or magnified depending on whether uv^{-1} is greater or smaller than unity) replica of the object amplitude. This result justifies computing images from (11) with FFT's of the measured data $u_o(y_h)$ multiplied by $\exp i(k/2)(v^{-1} - f^{-1})y_h^2$.

Calculations can also be based on the angular spectrum concept rather than the Fresnel approximation of scalar diffraction theory [3], [41], [52]. The angular spectrum computation is convenient because it also utilizes the FFT. In particular, it is useful when the object is close to the recording aperture; however, at large distances it has questionable utility because its computation requires more data than computation of the diffraction integral. The large amount of data is required because samples must be spaced by less than half the wavelength and because diffraction spreads the object wave.

The resolution enhancement furnished by simultaneously scanning the transmitter and receiver can be appreciated by comparing Figs. 15 and 16 [42]. The holograms shown in these figures are of the same test object, a toy pistol, and were recorded using the same wavelength of illumination ($\lambda = 4$ mm) and nearly equal f-number. The hologram in Fig. 15 was recorded by scanning the receiver only, while that shown in Fig. 16 was obtained by simultaneous scanning of transmitter and receiver. The resolution enhancement is suggested by the finer structure of the hologram and demonstrated by the

TABLE I
APPLICATIONS OF MICROWAVE HOLOGRAPHY

Applications	References
Airborne Imaging; Terrain Mapping, and Contouring	[53], [54]
Antenna Farfield Patterns	[55], [56]
Antenna Nearfield Distributions	[57]-[64]
Dielectrics: Anomalies and Structure	[65]-[70], [41], [43]
Hologram Antennas	[71]-[73]
Interferometric Analysis of Deformations	[32]-[34], [74]
Imaging Metallic Objects in Dielectrics	[35], [25], [38]
Radar Target Identification	[27], [75]
Radio Wave Propagation and Scattering	[76]-[81]
Radome Diagnostics	[82]-[83]

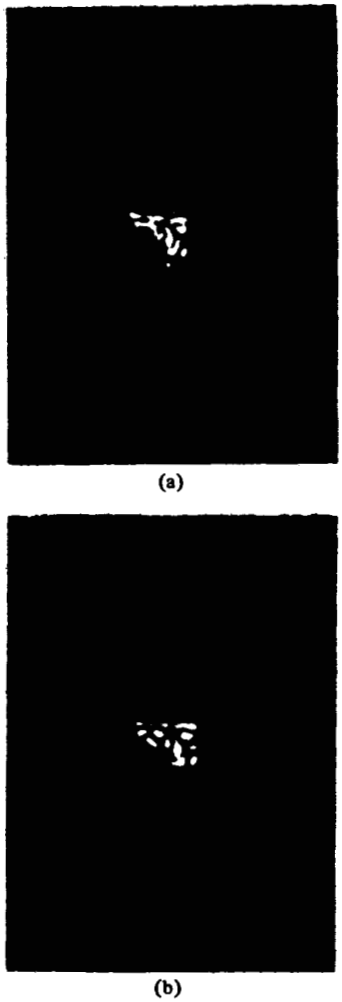

(a)

(b)

Fig. 17. Images produced by reconstruction directly with hologram (a); From Light-Valve Arrangement of Fig. 9, in (b)

closer resemblance of the image to the object. In instances of microwave imaging through partially lossy dielectrics such as soil or rock, absorption losses increase with decreasing wavelength. Thus a compromise between resolution and depth of penetration must be made. Simultaneous scanning is, therefore, particularly suited for such imaging conditions because the enhancement of resolution it affords does not involve decreasing wavelength [41].

The operation of the real-time reconstruction concept described in Fig. 9 has been demonstrated [49]. An optical transparency replica of a microwave hologram was used as a test hologram in the projection arm of Fig. 9 to address the image converter cell. Images of a toy pistol were produced by the image converter, and directly from the test hologram. The images, presented in Fig. 17, differ negligibly. In actual operation a light valve can be addressed by a CRT display of microwave hologram data or a LED display as in Fig. 6.

IV. APPLICATIONS

Microwave holography has many diverse applications. Some involve long distances; others involve small scale. Some applications require complex apparatus or controlled laboratory conditions, but holograms involving natural objects such as terrain or troposphere are also possible. The best known application is terrain mapping by SAR systems. Natural holograms occur, for example, when the troposphere or the Earth's surface scatter radio waves that interfere with waves directly from a transmitting antenna. The angles to the scatterers from the observing sight are computed from the measured interference pattern. In addition to the applications that involve long distances, microwave holography can image nearby objects in optically opaque dielectric regions. Examples include weapons concealed by clothing and anomalies in soil or solid propellants for rockets. Holographic methods also have been applied to measure fields near radiating antennas. Holograms can evaluate internal reflections in radomes without wavefront reconstruction and can be used in the synthesis of microwave antennas.

Table I lists several applications and gives references for each.[1] The nomenclature of the applications and the grouping of references emphasize the properties of the object being imaged or the data being sought in the tests. Although the references describe experiments that demonstrate feasibility, some of the applications should be considered potential because instruments and procedures are partially developed. The remainder of this section details the applications of microwave holography.

A. Airborne Microwave Holographic Radar

Larson *et al.* developed an airborne microwave holographic radar [53], [54] which differs from SAR because it emits continuous waves rather than pulses. However, like SAR it requires relative displacement of the antenna and the object. The radar has 100 receiving antennas in a linear array and a coherent receiver for each antenna. The signals from all antennas are time multiplexed and displayed by an oscillo-

[1] Table I omits synthetic aperture radar that utilizes pulsed radiations. The reasons for this omission were given in the Introduction.

scope and photographed to generate one dimension of a hologram. The orthogonal dimension is generated by moving the film during the aircraft's motion. Images are generated by optically processing the hologram. The system utilizes 16.8-GHz waves and has a field of view from directly below the aircraft to 45° on each side. Resolution in the direction of motion depends on the length of the synthesized aperture. Resolution in the transverse direction is $R\lambda/L$ where R is range, λ is wavelength, and L is array length. Typical values of range are 300 to 400 m.

The system has formed high quality images of objects and features on the Earth's surface. Unlike conventional cameras it can form images through fog, inclement weather, and at night. The system generates terrain height contours when it operates at two frequencies. A similar system in which the coherent array is stationary has been used successfully in the imaging of rotating objects [52].

B. Antennas, Far-Field Patterns

The far-field radiation pattern of a microwave antenna can be determined holographically [55]. Of course, far-field patterns can be measured directly so the reason for using holograms deserve comment. An antenna that is large in terms of wavelengths requires a long test range whose length R is determined by the farfield condition $2D^2/\lambda$; where D is antenna diameter, and λ is wavelength. For example, if D is 10 m and λ is 0.1 m, R is greater than 2000 m. Antenna test ranges of this length can be quite expensive and can have midrange reflections that cause errors. The holographic approach is to measure the field radiated by the antenna in the region of Fresnel diffraction and to compute the farfield patterns. The computation can be optical with a laser beam illuminating a transparency that represents the measured data; a photometer scanned transverse to the reconstructed optical antenna beam can give sections of the radiation pattern. The computation can also be digital; FFT algorithms have been used to reduce costs. Data economy in digital calculations has been studied recently in connection with antennas [56] and hologram sampling [37].

C. Antenna Near-Field Diagnostics

The holographic method can determine the field near a radiating antenna or diffracting aperture from measurements in either the Fraunhofer or Fresnel regions. The aperture field is useful because it connects features of the farfield pattern to the antenna's structure. For example, a feed antenna at the focus of a paraboloid can diffract and increase sidelobe levels. An additional objective is to locate defective elements in an array.

The holographic method gives a unique near-field distribution because it determines far-field phase; in contrast, a far-field intensity pattern would not uniquely specify the near-field distribution. Phase can be obtained even when only intensity is detected if a coherent reference wave is added to the radiation from the antenna being tested. Napier and Bates described a method that utilizes only power measurements with a second antenna that radiates the reference wave; they reconstructed computationally to determine the near-field distribution [57]–[60]. Iizuka and Gregoris have imaged a nine wavelength long monopole antenna; the reconstruction utilized laser light and holograms were formed by copying a microwave activated liquid crystal panel [24]. The image of the monopole, when resonant, showed brightness maxima at each end, suggesting the current distribution has maxima at the ends. A computational method for locating defective elements in array antennas was proposed and numerically simulated by Ransom and Mittra; the success in locating a defective element depended on the phase error between the element and its neighbors [61]. This result suggests a resolution limit in the method. Bennett *et al.* imaged the field near a radiating paraboloidal antenna from far-field measurements; blockage by a feed antenna was made visible [62]. The field near an antenna is also useful for analyzing the effect of a radome [63]. The near field is required for diffraction calculations, but the calculations require that the distribution be inside the radome. Laser light reconstructions from Fourier transform holograms have imaged active regions of log-periodic antennas. Near-field distributions of simple arrays have been computed from Fourier transform holograms by processing the detected intensity fringes in a low frequency, electronic spectrum analyzer. Antenna nearfields have also been computed digitally from measurement of phase and amplitude on a spherical surface [64]. A spherical surface reduces the effect of the receiving probe's pattern. This effect can be large for data measured on a planar surface; and requires therefore additional processing to determine the antenna near-field.

In this antenna application we can interpret the object as a current distribution or a nearfield distribution. Near fields have also been computed from measured data by backward propagation with an algorithm based on the angular spectrum concept; this work has not yet been published.

D. Dielectrics: Structures and Anomalies

Because microwaves propagate with slight attenuation through many optically opaque dielectric structures, microwave holographic imaging can locate internal anomalies. For example, relatively high microwave frequencies can be used to image imperfect bonds in laminated plastic components. The lower microwave frequencies can be used in geophysical and archeological explorations to locate voids buried in soil. Iizuka imaged thin flat voids of finite breadth inside flat dielectric layers with 34.26-GHz waves [65] employing a fixed antenna illuminator and a liquid crystal panel as area detector. Radiated power was high (15 W) and reflection at the smooth outer boundary generated the reference wave. Reconstructions with laser light from size-reduced holograms produced images. However, the images were somewhat obscured by additional overlapping images because the angle between the object and reference waves was small. Iizuka also has imaged a plasma and removed the obscuration caused by the glass bottle that contained the plasma by means of holographic subtraction [66]. Again the detector was a liquid crystal panel, but the frequency was 94 GHz; the radiated power was 5 W. Reconstructions were made optically from a reduced size copy of the millimeter-wave hologram.

Ogura and Iizuka have developed a helicopter-carried holographic radar designed to determine the thickness of ice layers [67], [68]. This radar is remarkable because it uses continuous wave radiation rather than pulses and because it has two linear antenna arrays. The antenna elements in the array are spaced quadratically, rather than uniformly, to transform the quadratically spaced fringes in a Fresnel zone plate to a linear spacing in a mathematical coordinate system that catalogs the measured data. One of the linear antenna arrays receives, while the antennas of the second array transmit sequentially. Data were gathered by all the receiving antennas during radi-

ation by each transmitting antenna to generate a matrix of data. The matrix, called a hologram matrix, is analogous to a scattering matrix. The data are computationally processed to form detection peaks which give ranges to the boundaries of the ice. A discussion of the differences between the hologram matrix radar and a stationary synthetic aperture radar has recently appeared [69]. The quadratic spacing in the arrays may be special to a specific range interval, but this point has apparently not been discussed.

In another work [43] small low-density dielectric rods obscured by a random microwave diffuser have been imaged. The bistatic apparatus had a fixed illuminating antenna and a scanned receiving probe. Frequency was 16 GHz. A network analyzer measured phase and amplitude. The data was encoded into detour-phase holograms which were size reduced and illuminated with laser light to form images. Image quality depended on whether the objects were on the illuminated or shadowed surface of the diffuser [70]. Yue and his colleagues imaged dielectric anomalies buried in soil [41] using a frequency of 2.5 GHz. A single antenna that received and transmitted simultaneously scanned the area of interest. Reconstructions were made in two ways. One was with laser light illuminating detour phase holograms. In this case the logarithm of the measured amplitude was encoded to suppress the reflection from the air–soil interface. The second method was computational with algorithms based on the angular spectrum concept. A coherent background was measured in the region without the void; substructing this background from the data in the region of the object enhanced images. Images from both reconstruction methods were improved when the soil surface was slightly roughened with surface deformations of random shape and depth less than about one-tenth wavelength.

E. Hologram Antennas

Microwave holograms for which the reconstruction is done with microwaves can be used as antennas. The hologram antenna is illuminated with microwaves from a small feed antenna, and the hologram diffracts to form the desired far-field pattern. The presence of unwanted diffracted orders can be overcome by constructing phase modulating holograms.

The microwave holograms are produced by recording or computing the interference pattern produced by the wavefield of a reference feed horn and the wavefield of the desired master antenna. The interference pattern is determined over a plane surface or a surface of arbitrary shape. Once the interference pattern is determined, one can construct the microwave hologram antenna. Checcacci *et al.* [71], [72] studied three techniques for constructing the microwave hologram: Holograms in which the fringe pattern is encoded as variable phase modulation; binary transmittance holograms in which the fringe widths are retained; and binary holograms in which only the fringe periodicity is retained. Because microwave hologram antennas can be formed on an arbitrary surface, they have promise in conformal antenna design for aerospace applications.

More recently Iizuka *et al.* developed a volume-type hologram antenna which is comprised of two planar parallel holograms [73]. A small antenna between the holograms radiates in their plane. Each hologram consists of concentric circles, but corresponding radii of the circles in the two holograms differ by a quarter wavelength. The quarter wave differences produce a farfield pattern that has a maximum on one side of the antenna and a minimum on the opposite side. Kock has pointed out that metal-plate microwave lenses can be interpreted as holograms. Some early Gabor-type microwave holograms were utilized to simulate far-field diffraction of radomes, but the holograms developed for this application were not designed to be efficient antennas.

F. Holographic Interferometry

Deformations of stressed bodies have been studied with optical holograms, and some work has been done with microwave holograms to study objects too large for the optical technique. This work was done by Papi, *et al.* at the University of Florence [32], [33]. They deformed a large plate and made holograms with 9.375-GHz waves. Their technique utilized double exposures. The images formed by reconstructing with laser light showed considerable speckle. More recently the same authors described a two-frequency method of microwave interferometry [34].

Holographic interferometry has been utilized by Ginzburg *et al.* to determine the dielectric constant of a large sample [74]. This application of microwave holography seems to have potential, but it is not as well developed as some of the others.

G. Imaging Metallic Objects in Optically Opaque Dielectric Regions

Airline hijacking stimulated the development of methods for detecting concealed weapons. Although laboratory experiments demonstrated the feasibility of microwave holographic imaging for this application, no systems have been developed for use at airports. Radio frequency metal detectors and X-ray machines are the accepted devices for screening passengers and luggage because they are cheaper and more effective. Nevertheless the thrust for concealed weapons detection stimulated the development of microwave holography. It seems that outdoor applications exist that require relatively low frequencies and that permit only backscattering measurements. Examples of this sort are buried pipes and cables.

The earliest work on imaging concealed weapons appears to be that of Farhat and Guard, who imaged a pistol concealed by clothing and leather [35]. They utilized 70-GHz continuous waves and phase-locked receiver to form phase-only holograms. Images were formed with laser light from scale-reduced holograms. Data were collected by spiral scanning the receiving antenna over the recording aperture. An example in the test hologram is shown in [49]. The elaborate hologram was recorded through a layer of heavy clothing. The reconstructed image is shown in Fig. 17. Spatial filtering of zeroth-order light was employed to remove background light in the image plane and thus enhance image quality.

Kock proposed a real-time method for imaging metallic objects [25]. The approach is to record the field scattered by an object with a liquid crystal panel. The recording film would be close to the object so its geometric optical projection would be recorded. No reconstruction would be required. The intensity levels required by this approach may be unacceptably high.

Orme and Anderson imaged metallic objects in dielectric surrounding with 34.88-GHz waves [38]. Their novel apparatus uses one antenna to illuminate the object and a rotating dipole antenna to receive the object field. The dipole and illuminator are scanned together to improve resolution. The phase of the reference wave is linearly changed with probe position to simulate an offset reference beam so images are displaced laterally from undiffracted light during reconstruction.

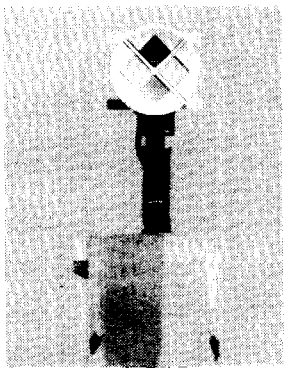

(a)

(b)

Fig. 18. Paraboloidal reflector (a) and image (b). The pattern on the reflector is colored paint to show its orientation when used as a polarized antenna.

The phase shift is produced by radiating the reference beam from an antenna on the probe carriage toward a large fixed reflector and mixing the reflected reference wave with the object scattered wave.

H. Radar Target Identification

Dooley described one of the earliest experiments in which images of a microwave illuminated target were produced [27]. In this experiment Gabor type holograms were formed with 3-cm waves. The fields reflected from a radar target were measured by a scanning probe over the hologram aperture and displaying the hologram data on an oscilloscope. Holograms were formed by photographing the display and scale reducing the photograph. Reconstruction was made with laser light.

An electronic method for imaging radar targets was developed by Waters and Eikenberg [75]. They utilized a transmitting antenna and an array of 128 receiving antennas. The system electronically scanned the pattern of the array and combined the received signals. The received power was displayed on an oscilloscope to form images. A wavefront reconstruction radar system was described in a 1966 patent issued to K. F. Ross, but no published data on a system seem to exist. Farhat has recently suggested imaging with a large circular array. The method would use target motion to synthesize an imaging aperture and correct for irrotational target maneuvers [42].

Another holographic method for imaging has been developed with two orthogonal linear arrays; see Fig. 5. This array was developed for short-range imaging and for scattering diagnostics. An image of a paraboloidal antenna obtained with the system is shown in Fig. 18. The image is a composite formed by superimposing several images for distinct object orientations to reduce speckle [40].

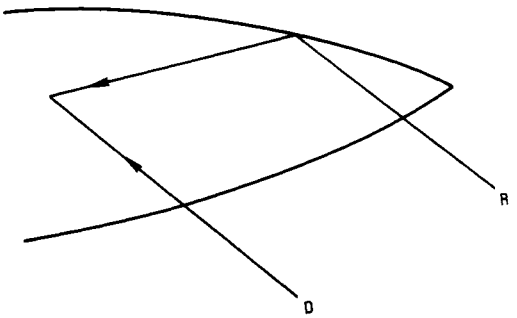

Fig. 19. Interference between a direct wave D and a reflected wave R in a radome shell.

I. Radio Wave Propagation

The earliest application of microwave holography was to the imaging of ionospheric layers. Rogers suggested this application in 1956 and gave additional verification in 1957 [76]–[78]. The idea was to measure, using three receiving antennas, 2.404-MHz waves that were reflected from the ionosphere. The reflected intensities were converted to variable density film transparencies; i.e., holograms. Images were produced by illuminating the holograms with laser light. The images retrieved were related to movement of ionospheric layers.

One of the most recently published applications of microwave holography is in locating reflecting regions of the troposphere or Earth's surface [79]. Ja has described measurements of the angles of arrival of 4 GHz waves [80]. Holograms are formed by the interference of waves that are scattered by the troposphere, reflected by the Earth, and propagated directly from the transmitter. The fringe pattern was measured by an antenna that moved vertically on a mast 85 m tall. The formation step would be familiar to propagation scientists as a height gain measurement. The hologram pattern is computationally analyzed to determine angles of arrival and hence the directions of scatterers. Microwave holograms also are formed by interference between the direct wave and wave reflected from water surfaces. Some unpublished measurements have imaged wind-generated water waves [81].

J. Radomes

A radar antenna carried by a fast airplane is usually placed in a streamlined dielectric shell, a radome, to protect the antenna and preserve the aerodynamic contour. Although necessary, radomes produce undesirable effects. They attenuate radar waves, cause errors in angular measurements, and distort antenna patterns. These effects can be explained by examining the wavefronts produced in the radome-bounded region by externally incident plane waves. The wavefronts depart from plane waves; these departures are phase aberrations. The intensity also can be nonuniform because of reflections like those suggested in Fig. 19. The reflections also increase the levels of sidelobes in antenna patterns.

Microwave holography is particularly suitable for studying reflections in radomes because the reflections generate holograms.[2] The reflected wave in Fig. 19 interferes with the wave

[2] Radome reflections occur only for a limited range of directions of the incident wave. The angle between the wave normal and the radome axis must exceed the local slope of the radome contour. At relatively small angles, the tip of the radome scatters a field that has small magnitude but significant effect on angular error. This topic is being studied with microwave holography.

(a) (b)

Fig. 20. Hologram (a) formed by radome reflections and conjugate images (b) of the reflecting region.

propagated directly through the radome. Holograms can be formed by detecting the fringe pattern, displaying it on an oscilloscope, and scale-reducing a photograph of the display. The almost uniform direct wave is the reference wave and the reflected wave is the object wave. Fig. 20 (a) shows a hologram formed inside a nearly concial radome. The reconstruction of this hologram also shown in Fig. 20(b) shows two crescent shaped images of the reflecting region. In practical applications, the images locate the portions of the radome that cause reflections. The thickness of the reflecting portions of the radome are changed to reduce reflected intensity, which can be monitored by monitoring the fringe contrast directly [82], [83].

V. Conclusions

The extension of holography to the microwave region leads to novel applications in the analysis and synthesis of antennas, nondestructive testing, ionospheric and tropospheric mapping and radar. Practical use of some of these methods depends on the development of rapid recording, processing and reconstruction techniques. Advances in all three areas are being made.

References

[1] D. Gabor, "A new microscopic principle," *Nature*, vol. 161, no. 4098, pp. 777–778, 1948.
[2] E. N. Leith and J. Upatnieks, *J. Opt. Soc. Amer.*
[3] J. N. Goodman, *Introduction to Fourier Optics*. New York: McGraw-Hill, 1968, Ch. 8.
[4] G. W. Stroke, *An Introduction to Coherent Optics and Holography*. New York: Academic Press, 1966.
[5] H. M. Smith, *Principles of Holography*. New York: Wiley-Interscience, 1970.
[6] H. J. Caulfield and S. Lu, *The Applications of Holography*. New York: Wiley-Interscience, 1970.
[7] R. J. Collier, C. B. Burkhardt, and L. H. Lin, *Optical Holography*. New York: Academic Press, 1970.
[8] M. Francon, *Holography*. New York: Academic Press, 1974 (English translation from the French edition, *Holographie*).
[9] A. F. Metherell, H. M. A. El-Sum, and L. Larmore, Eds., *Acoustical Holography*. New York: Plenum Press, 1969, vol. 1.
[10] A. F. Metherell and L. Larmore, Eds., *Acoustical Holography*. New York: Plenum Press, 1970, vol. 2.
[11] A. F. Metherell, Ed., *Acoustical Holography*. New York: Plenum Press, 1971, vol. 3.
[12] G. Wade, Ed., *Acoustical Holography*. New York: Plenum Press, 1972, vol. 4.
[13] P. S. Green, Ed., *Acoustical Holography*. New York: Plenum Press, 1974, vol. 5.
[14] N. Booth, Ed., *Acoustical Holography*. New York: Plenum Press, 1975, vol. 6.
[15] R. K. Mueller and N. H. Farhat, Ed., "Acoustical holography survey," *Advances in Holography*. New York: M. Dekker, 1975, vol. 1.
[16] B. P. Hildebrand and B. B. Brenden, *An Introduction to Acoustical Holography*. New York: Plenum Press, 1972, ch. 4.
[17] E. N. Leith, "Quasi-holographic techniques in the microwave region," *Proc. IEEE* vol. 59, pp. 1305–1318, 1969.
[18] R. O. Harger, *Synthetic Aperture Radar Systems: Theory and Design*. New York: Academic Press, 1970.
[19] L. J. Cutrona and G. O. Hall, "A comparison of methods for achieving fine azimuth Resolution," *IRE Trans.*, vol. MIL-G, pp. 119–121, 1962.
[20] W. E. Kock, "Stationary coherent (hologram) radar and sonar," *Proc. IEEE*, vol. 56, pp. 2180–2181, 1968.
[21] C. F. Augustine, "Field detector works in real time," *Electronics*, vol. 41, pp. 118–121, 1968.
[22] C. F. Augustine, C. Deutsch, D. Fritzler, and E. Marom, "Microwave holography using liquid crystal area detectors," *Proc. IEEE*, vol. 57, p. 1333, 1969.
[23] H. E. Stockman and B. Zarwyn, *Proc. IEEE*, vol. 56, p. 763, 1968.
[24] K. Iizuka and L. G. Gregoris, "Application of microwave holography in the study of the field from a radiating source." *Appl. Phys. Lett.*, vol. 17, pp. 509–512, 1970.
[25] W. E. Kock, "Real-time detection of metallic objects using liquid crystal microwave holograms," *Proc. IEEE*, vol. 60, p. 1104, 1972.
[26] K. Iizuka, "Microwave holography by photoengraving," *Proc. IEEE*, vol. 57, pp. 812–814, 1969.
[27] R. P. Dooley, "X-band holography," *Proc. IEEE*, vol. 53, p. 1573, 1965.
[28] G. Tricoles and E. L. Rope, *J. Opt. Soc. Amer.*, vol. 56, p. 542, 1966.
[29] —, "Reconstructions of visible images from reduced-scale replicas of microwave holograms," *J. Opt. Soc. Amer.*, vol. 57, pp. 97–99, 1967.
[30] Y. Aoki, *Appl. Opt.*, vol. 6, p. 1943, 1967.
[31] —, "Microwave holography by a two beam interference method," *Proc. IEEE*, vol. 56, p. 1402, 1968.
[32] G. Papi, V. Russo, and S. Sottini, "Optical wave reconstruction from microwave holograms and applications to interferometry," *Applications of Holography*, J.-Ch. Vienot, Ed., University of Besancon, France, 1970.
[33] —, "Microwave holographic interferometry," *IEEE Trans. Antennas Propagat.* vol. AP-19, p. 740, 1971.
[34] —, "Two frequency microwave holographic interferometry," *Proc. IEEE*, vol. 60, pp. 1004–1005, 1972.
[35] N. H. Farhat and W. Guard, "Millimeter wave imaging of concealed weapons," *Proc. IEEE*, vol. 59, pp. 1383–1384, 1971.
[36] N. H. Farhat and A. H. Farhat, "Double circular scan in microwave holography," *Proc. IEEE*, vol. 61, pp. 509–510, 1973.
[37] A. W. Lohmann, "Data economy in holography," *J. Opt. Soc. Amer.*, vol. 59, p. 482, 1969.
[38] R. D. Orme and A. P. Anderson, "High resolution microwave holographic techniques," *Proc. Inst. Elec. Eng.*, vol. 120, pp. 401–404, 1973.
[39] W. Wells, "Conical holography" in *Acoustical Holography*, vol. 2, A. F. Metherell and L. Larmore, Eds. New York: Plenum Press, 1970.
[40] R. A. Hayward, E. L. Rope, G. Tricoles, and O-C. Yue, "Enhancement by noncoherent superposition of microwave images formed with crossed, coherent arrays," *Acoustical Holography*, vol. 6, N. Booth, Ed.
[41] O.-C. Yue, G. Tricoles, E. L. Rope, "Two reconstruction methods for microwave imaging of buried dielectric anomalies," IEEE Trans. *Comput.*, vol. C-24, pp. 381–390, 1975, also summarized in *Dig. IEEE Optical Computing Conf.*, 1974.
[42] N. Farhat, "High resolution microwave holography and the imaging of remote objects," *Optical Engineering*, vol. 14, pp. 499–505, 1975.
[43] E. L. Rope and G. Tricoles, "Microwave Holography: Difussers; Binary Detour-Phase Holography," *Applications of Holography*, J-Ch. Vienot, Ed., University of Besancon, 1970.
[44] W. E. Kock and F. K. Harvey, "Sound wave and microwave space patterns," *Bell. Syst. Tech. J.*, vol. 20, p. 564, 1951.
[45] N. H. Farhat and N. S. Kopeika, "A low-cost millimeter-wave glow discharge detector," *Proc. IEEE* (Lett.), vol. 60, pp. 759–760, 1972.
[46] S. G. Lipson, "Recyclable incoherent-to-coherent image converters," *Advances in Holography*, vol. 2, N. H. Farhat, Ed., M. Dekker Inc., New York, 1976.
[47] R. W. Meier, "Magnification and third order aberrations in holography," *J. Opt. Soc. Am.*, vol. 55, p. 978, 1965.
[48] W. T. Cathey, *Optical Information Processing and Holography*, New York: Wiley, 1974, pp. 345–347.
[49] M. Wu and N. H. Farhat, "Real-time optical reconstruction of microwave holograms," *Proc. IEEE* (Lett.), vol. 63, pp. 1254–1255, Aug. 1975.
[50] J. Goodman, "Digital image formation from detected hologram data," *Acoustical Holography*, vol. 1, A. F. Metherell, H. M. A. El-Sum, and L. Larmore, Eds. Plenum Press, pp. 173–184, 1969.
[51] Y. Aoki and A. Boivin, "Computer reconstruction of images from microwave holograms," *Proc. IEEE*, vol. 58, pp. 821–822, 1970.
[52] H. G. Booker and P. C. Clemmow, "The concept of an angular spectrum of plane waves, and its relation to that of a polar diagram and aperture distribution," *J. IEEE*, vol. 97, part III, pp. 11–17, 1950.
[53] R. W. Larson, J. S. Zelenka, and E. Johansen, "Microwave holography," *Proc. IEEE*, vol. 57, pp. 2162–2164, 1969.
[54] R. W. Larson, J. S. Zelenka, and E. Johansen, "A microwave hologram radar system," *IEEE Trans. Aerosp. Electron. Syst.*, vol. AES-8, pp. 208–217, 1972.
[55] L. D. Bakrakh, A. P. Kurochkin, and J. S. Hartunian, "The appli-

cation of holography to design and measuring of the parameters of high-directional antennas," *Applications of Holography*, J. Ch. Vienot, Ed., Besancon University, France, 1970.
[56] E. B. Joy and D. T. Paris, "Spatial sampling and filtering in near-field measurement," *IEEE Trans. Antennas Propagat.*, vol. AP-20, pp. 253-261, May 1972.
[57] R. H. T. Bates and P. J. Napier, "A suggestion for determining antenna pattern phase from holographic type measurement," *Proc. IREE*, Australia, vol. 32, pp. 164-166, 1971.
[58] P. J. Napier, "Array element modulus and phase from measured radiation patterns," *Proc. IREE*, Australia, vol. 32, pp. 466-468, 1971.
[59] P. J. Napier, and R. H. T. Bates, "Antenna aperture distributions from holographic type radiation pattern measurement," *Proc. IEEE*, vol. 120, pp. 30-34, 1973.
[60] R. H. T. Bates, "Holographic approach to radiation pattern measurement I, General Theory," *Inst. J. Eng, Sci.*, vol. 19, pp. 1107-1121, 1971.
[61] P. L. Ransom and R. Mittra, "A method for locating defective elements in large phased arrays," *Proc. IEEE*, vol. 59, pp. 1029-1030, 1971.
[62] J. C. Bennet, A. P. Anderson, P. A. McInnes, and A. J. T. Whittaker, "Conversion of farfield patterns of antennas to nearfield," *Digest IEEE, G-AP Symp. (1973)*. Also "Microwave holographic metrology of large reflector antennas," *IEEE Trans. Antennas Propagat.*, vol. AP-24, May 1976.
[63] E. L. Rope and G. Tricoles, "Microwave and optical holography as diagnostic methods for antennas and radomes," *IEEE Quantum Electron.*, vol. QE-5, 1969, abstract.
[64] E. L. Rope, R. A. Hayward, and G. Tricoles, "A holographic method for determining antenna nearfield distributions from measurement on a spherical surface," *Digest IEEE, G-AP Symp. (1973)*.
[65] K. Iizuka, "Visualization of internal structure by microwave holography," *Proc. IEEE*, vol. 58, p. 791, 1970.
[66] —, "Subtractive microwave holography and its application to plasma studies," *Appl. Phys. Lett.*, vol. 17, pp. 27-29, 1972.
[67] H. Ogura and K. Iizuka, "Hologram matrix and its application to a novel radar," *Proc. IEEE*, vol. 61, pp. 1040-1041, 1973.
[68] —, "Holographic ice survey system," *Design News*, p. 19, July 8, 1974.
[69] H. Ogura, K. Iizuka, and W. E. Kock; "Comments on hologram matrix and its application to a novel radar," *Proc. IEEE*, vol. 62, pp. 862-863, 1974.
[70] G. Tricoles and E. L. Rope, "Two microwave experiments and the possibility of a holographic model of the retina," *Holography and Medicine*, P. Greguss, Ed., IPC Science and Technology Press, pp. 120-123, 1975.
[71] P. F. Checcacci, V. Russo, A. M. Scheggi, "Holographic antennas," *Proc. IEEE*, vol. 56, pp. 2165-2167, 1968.
[72] P. F. Checcacci, G. P. Papi, V. Russo, "Holographic VHF antennas," *IEEE Trans. Antennas Propagat.* vol. AP-19, pp. 278-279, 1971.
[73] K. Iizuka, M. Mizusawa, S. Urasaki, H. Ushigome, "Volume type hologram antennas," *IEEE Antennas Propagat.*, vol. AP-23, pp. 807-810, 1975.
[74] V. M. Ginzburg, V. M. Meschankin, G. J. Ruckman, and B. M. Stepanov, "Microwave holographic interferometry" *Applications of Holography*, J-Ch. Vienot, Ed., University of Besancon, France, 1970.
[75] W. M. Waters and A. F. Eikenberg, "On the design of a large aperture radar for target imaging," *IEEE Trans. Aerosp. Electron. Syst.*, vol. AES-4, pp. 886-892, 1968.
[76] G. L. Rogers, "A new method of analyzing ionospheric movement records," *Nature*, vol. 177, pp. 613-614, 1956.
[77] —, "Diffraction microscopy and the ionosphere" *J. Atmos. Terr. Phys.*, vol. 10, pp. 332-337, 1957.
[78] G. L. Rogers, "An experimental verificational diffraction microscopy, using radio waves," *J. Atmos. Terr. Phys.*, vol. 11, pp. 51-53, 1975.
[79] Y. H. Ja, "Measurement of angles of arrival by microwave holographic Techniques," *IEEE Trans. Antennas Propagat.*, vol. AP-23, pp. 720-722, 1975.
[80] Y. H. Ja, "Holographic reconstruction of source distributions from microwave height gain curves," *IEEE Trans. Antennas Propagat.*, vol. AP-24, pp. 4-5, 1976.
[81] E. L. Rope, G. Tricoles, O.-C. Yue, "Passive location by microwave holography," *General Dynamics Electronics Division Report*, R73-074-4, May 1974.
[82] G. Tricoles and E. L. Rope, "Applications of microwave holography to radomes and antennas," in *Digest IEEE, G-AP Symposium, 1971*.
[83] E. L. Rope and G. Tricoles, "Microwave holography applied to hollow dielectric shells," *J. Opt. Soc. Amer.*, vol. 61, p. 1571, 1971.

Incoherent Optical Correlators

MICHAEL A. MONAHAN, KEITH BROMLEY, AND RICHARD P. BOCKER

Abstract—**The use of optical systems in signal processing applications can offer significant advantages over an equivalent electronic approach. These advantages stem chiefly from the high-speed analog multiply and parallel processing capability inherent in an optical system. This can be used to advantage in application areas requiring large quantities of data to be processed in near real time. Presented in this paper is a review of a variety of incoherent optical analog techniques for performing correlation and linear transform operations. Both scanning and nonscanning systems using spatial and/or temporal inputs are considered.**

I. Introduction

WE CONSIDER in the following pages a wide variety of incoherent optical processing systems designed to perform an even wider variety of signal processing computations.[1] The emphasis here is placed exclusively upon optical systems with *incoherent* light sources. This distinguishes them from coherent processing systems widely discussed in the literature and for which several excellent survey papers have been written [1]-[7]. The basic attraction for coherent optical processing systems is that when the light source is coherent (e.g., a gas laser), a two-dimensional Fourier transform relation exists between the front and rear focal planes of a lens used in such a system. Because of this Fourier transform relation, operations can be performed in the (spatial) frequency domain. Therefore, coherent optical processing systems are somewhat analogous to electrical filters and find natural application in areas such as spectrum analysis, pattern recognition, and image processing.

On the other hand, an incoherent optical system possesses no such Fourier transform relation and operations are all done in the spatial domain. Nonetheless, incoherent optical systems find widespread application in a number of signal processing areas, many of which will be described in this paper. Without exception, the operation of each system or approach to be discussed can be described by a general linear transformation in

Manuscript received March 12, 1976.
The authors are with the Naval Electronics Laboratory Center, Electrooptics and Optics Division, San Diego, CA 92152.
[1] As in any review paper, omissions have undoubtedly occurred. To those whose works have been somehow overlooked, the authors offer their apologies. We would appreciate any criticisms or additions so that these may be incorporated into subsequent reviews of the field.

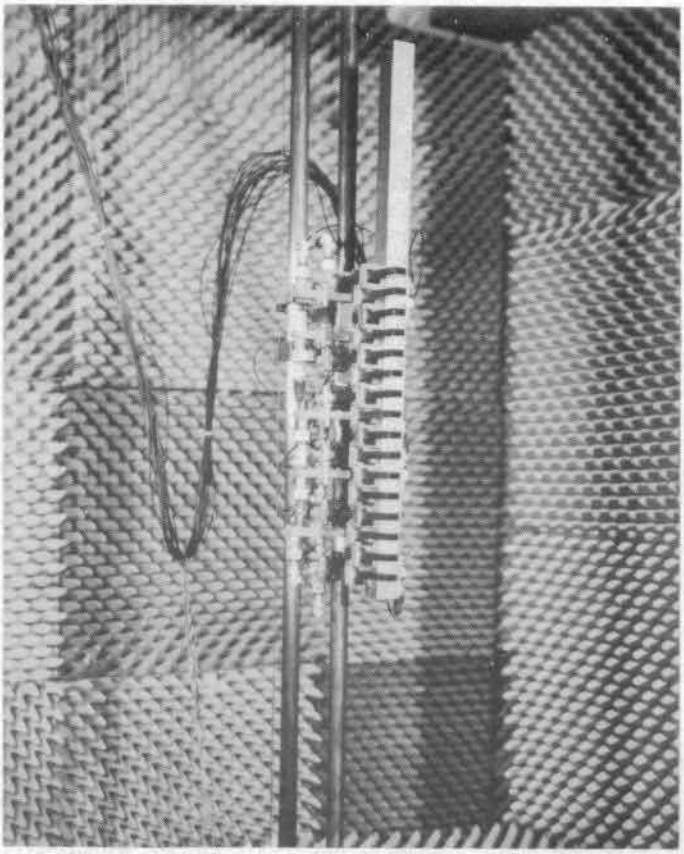

Fig. 4. Linear array for intensity measurements. The array is translated horizontally to scan an area.

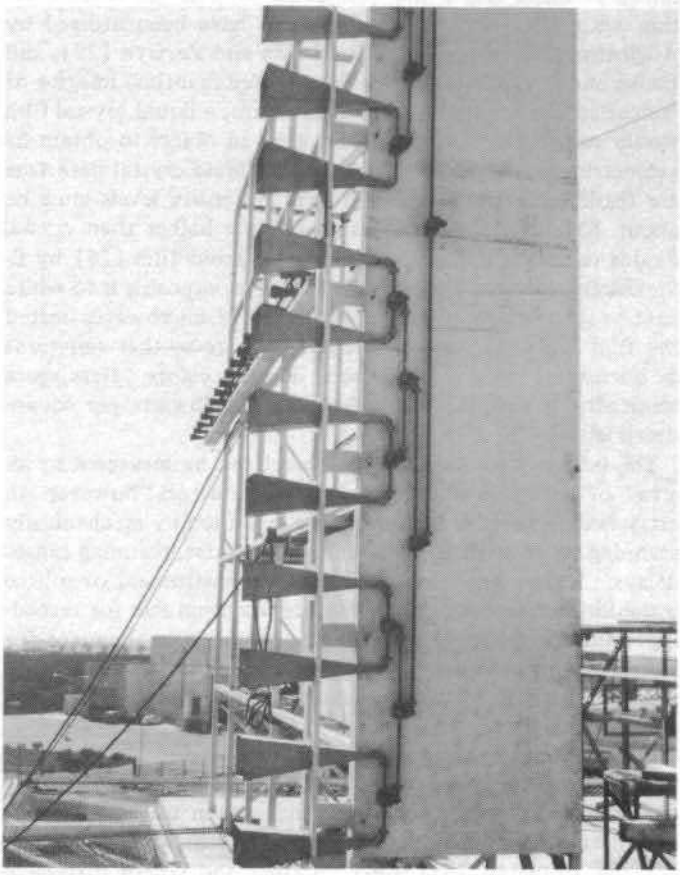

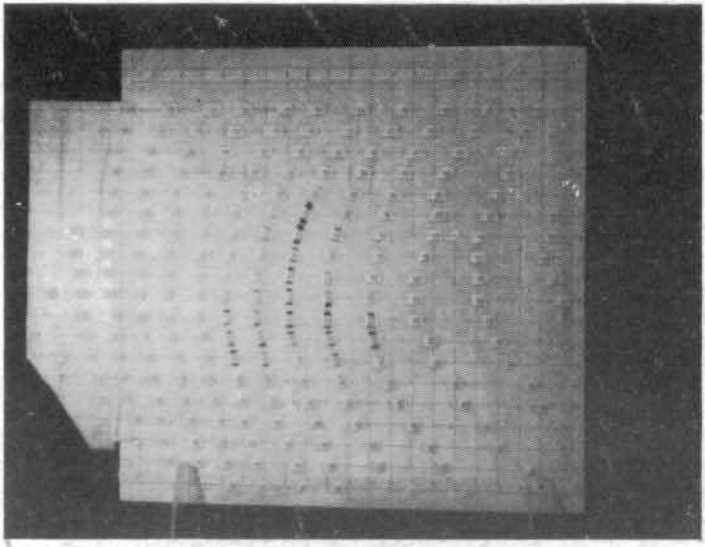

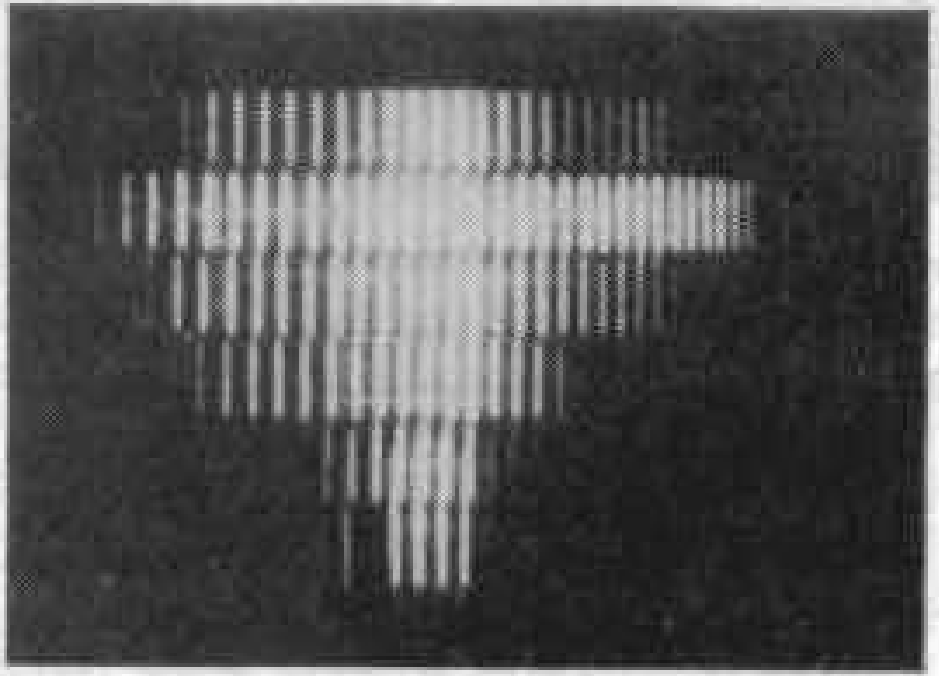

Fig. 11. Image of the object in Fig. 1 produced by illuminating the hologram in Fig. 8 with microwaves.

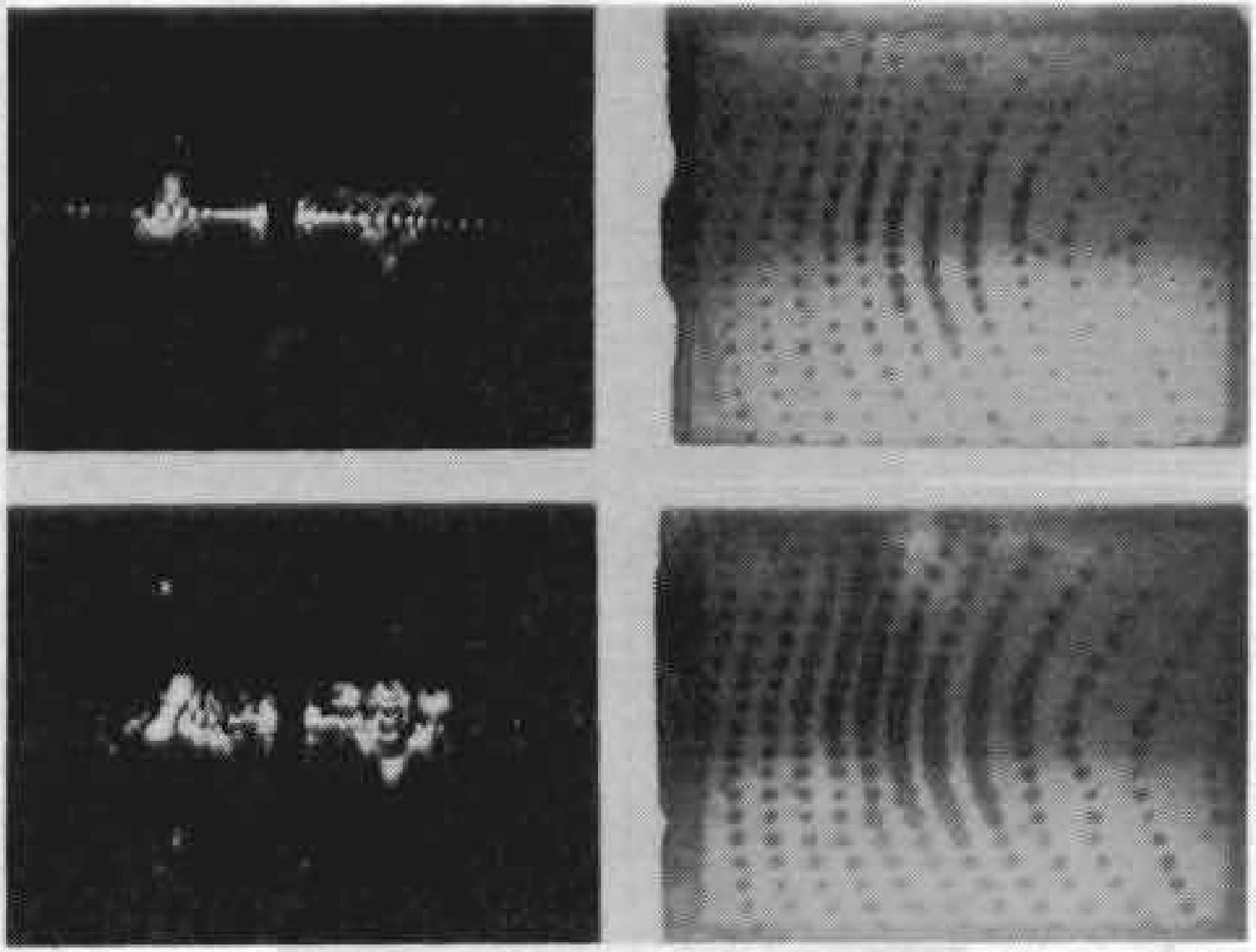

Fig. 12. Visible reconstructions of the triangular aperture in Fig. 1 and microscope photographs of holograms. The holograms differ in the exposures utilized in the photographic scale reduction. The upper [illegible] between holograms and reconstructions is horizontal.

(a)

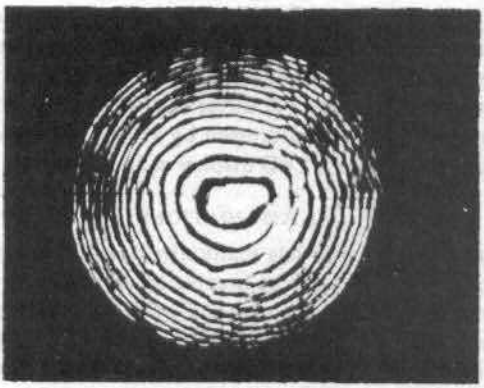

(b)

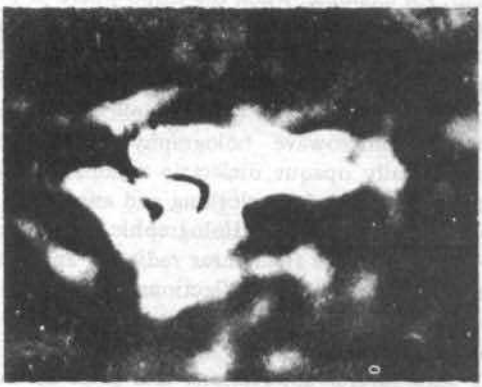

(c)

Fig. 15. Conventional scanned receiver holography. (a) Test object, (b) hologram, and (c) image.

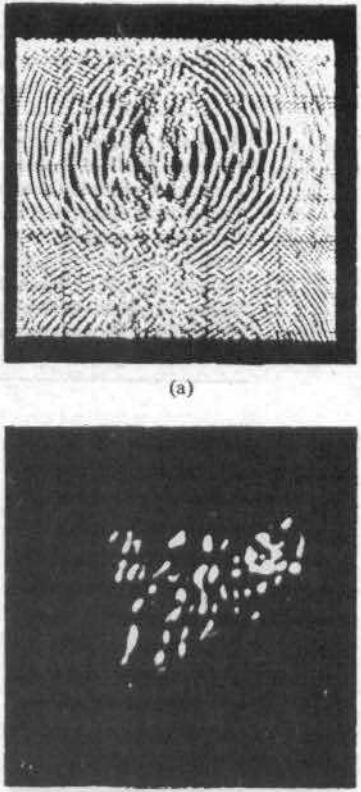

(a)

(b)

Fig. 16. Holography for simultaneously scanned receiver–Transmitter. The object is in Fig. 15, a) is the hologram, and b) is the image.

(a)

(b)

Fig. 17. Images produced by reconstruction directly with hologram (a);

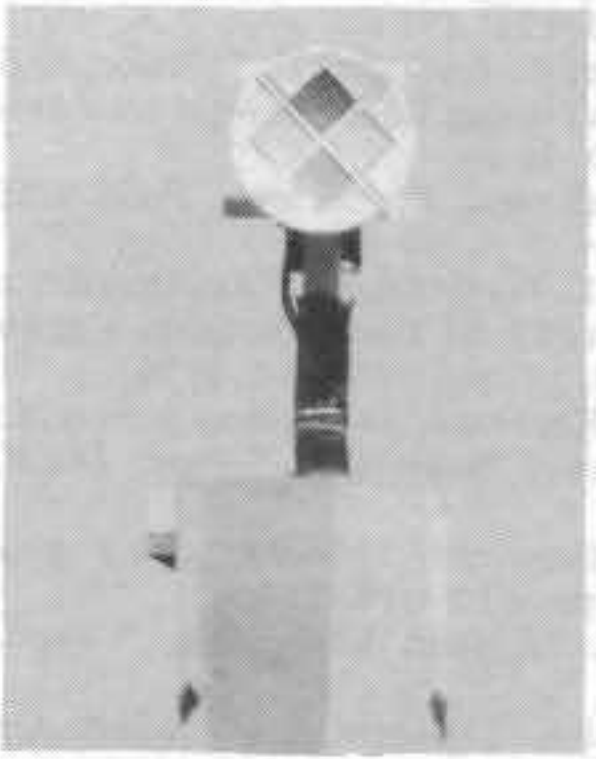

(a)

(b)

Fig. 18. Paraboloidal reflector (a) and image (b). The pattern on the reflector is colored paint to show its orientation when used as a polarized antenna.

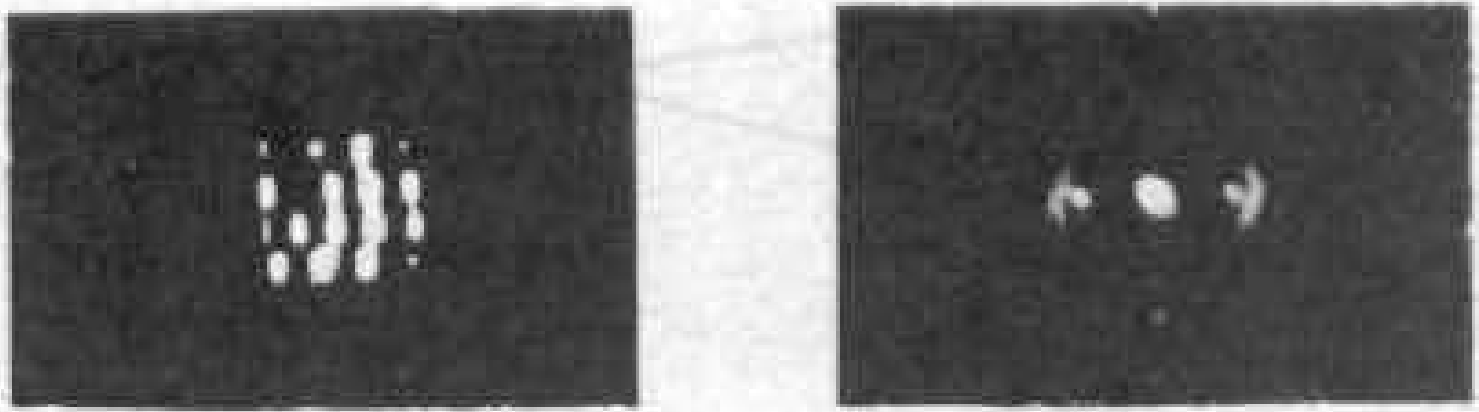

(a) (b)

Fig. 20. Hologram (a) formed by random reflections and conjugate images (b) of the reflecting region.